HHS Public Access

Author manuscript

Nature. Author manuscript; available in PMC 2011 March 16.

Published in final edited form as:

Nature. 2010 March 11; 464(7286): 292–296. doi:10.1038/nature08792.

Telomere elongation in induced pluripotent stem cells from dyskeratosis congenita patients

Suneet Agarwal[1], **Yuin-Han Loh**[1], **Erin M. McLoughlin**[1], **Junjiu Huang**[2,3], **In-Hyun Park**[1], **Justine D. Miller**[1], **Hongguang Huo**[1], **Maja Okuka**[2], **Rosana Maria dos Reis**[2], **Sabine Loewer**[1], **Huck-Hui Ng**[4], **David L. Keefe**[2], **Frederick D. Goldman**[5], **Aloysius J. Klingelhutz**[6], **Lin Liu**[2,7], and **George Q. Daley**[1,8,9]

[1]Division of Hematology/Oncology, Children's Hospital Boston; Pediatric Oncology, Dana Farber Cancer Institute; Department of Biological Chemistry and Molecular Pharmacology, Harvard Medical School; Division of Hematology, Brigham and Women's Hospital; Harvard Stem Cell Institute; Manton Center for Orphan Diseases; Boston, MA USA

[2]Department of Obstetrics and Gynecology, University of South Florida College of Medicine, Tampa, FL USA

[3]School of Life Sciences, Sun Yat-sen University, Guangzhou, China

[4]Gene Regulatory Laboratory, Genome Institute of Singapore; Department of Biological Sciences, National University of Singapore; Singapore

[5]Department of Pediatrics, University of Iowa, Iowa City, IA USA

[6]Department of Microbiology, University of Iowa, Iowa City, IA USA

[7]College of Life Sciences, Nankai University, Tianjin, China

[8]Howard Hughes Medical Institute, Children's Hospital Boston, Boston, MA USA

Abstract

Patients with dyskeratosis congenita (DC), a disorder of telomere maintenance, suffer degeneration of multiple tissues[1–3]. Patient-specific induced pluripotent stem (iPS) cells[4] represent invaluable *in vitro* models for human degenerative disorders like DC. A cardinal feature of iPS cells is acquisition of indefinite self-renewal capacity, which is accompanied by induction of telomerase reverse transcriptase (*TERT*)[5–7]. We investigated whether defects in telomerase function would limit derivation and maintenance of iPS cells from patients with DC. Here we show that reprogrammed DC cells overcome a critical limitation in telomerase RNA component (*TERC*) levels to restore telomere maintenance and self-renewal. We discovered that *TERC*

[9]Correspondence: George.Daley@childrens.harvard.edu.

Author contributions S.A. (project planning, experimental work, data interpretation, preparation of manuscript); Y.H.L., I.H.P., J.H., E.M.M., J.D.M., R.M.R., M.O., H.H., S.L. (experimental work); H.-H.N., F.D.G., D.L.K., A.J.K., L.L., G.Q.D. (project planning, data interpretation, preparation of manuscript).

Full Methods and any associated references are available in the online version of the paper at www.nature.com/nature.

Supplementary Information is linked to the online version of the paper at www.nature.com/nature.

upregulation is a feature of the pluripotent state, that multiple telomerase components are targeted by pluripotency-associated transcription factors, and that in autosomal dominant DC, transcriptional silencing accompanies a 3' deletion at the *TERC* locus. Our results demonstrate that reprogramming restores telomere elongation in DC cells despite genetic lesions affecting telomerase, and suggest that strategies to increase *TERC* expression may be therapeutically beneficial in DC patients.

Reprogramming of somatic cells to a state of pluripotency is characterized by prolonged self-renewal, implying induction of telomere maintenance mechanisms. Recently, it was reported that reprogramming of mouse cells was accompanied by elongation of telomeres[8], but given the significant differences in telomere length and telomerase regulation in mouse and human cells, we asked whether normal human cells displayed telomere elongation after reprogramming. We generated iPS cell lines by retroviral transduction of primary human fibroblasts with the factors *Oct4*, *Sox2*, *Klf4*, and *c-Myc*, confirmed the pluripotent phenotype by gene expression and functional analysis[4], and determined the mean terminal restriction fragment (TRF) length of the donor fibroblast lines and corresponding iPS lines by Southern blot. We found that mean TRF length and total telomeric DNA was increased in iPS lines relative to the parental fibroblasts (Supplementary Fig. 1a). Similar findings using retrovirally-marked single-cell fibroblast sub-clones[5] argued against the notion that cells with long telomeres are uniquely susceptible to reprogramming (Supplementary Fig. 1b). Induction of *TERT* expression and telomerase activity correlated with reprogramming to pluripotency as previously shown[5]–[7] (Supplementary Figs. 1c–e). These data establish that direct factor-based reprogramming of human somatic cells results in net telomere elongation.

X-linked DC is caused by mutations in the dyskerin gene (*DKC1*)[9] which encodes an RNA binding protein whose inactivation destabilizes levels of *TERC*, resulting in shortened telomeres and premature senescence in patient cell lines[10],[11]. We asked whether a *DKC1* mutant fibroblast line (del37L[9]–[11]) could be reprogrammed and propagated in a pluripotent state. Compared to normal cells, the reprogramming efficiency of del37L cells was poor, yielding only 2–5 colonies from 10^5 input cells with a delayed latency (Supplementary Table 1). Nevertheless, *DKC1* mutant iPS colonies showed all hallmarks of pluripotency, including characteristic morphology (Fig. 1a), gene expression (Fig. 1b; Supplementary Fig. 2a), and formation of teratomas comprised of all three embryonic germ layers (Fig. 1c). PCR restriction fragment length polymorphism (RFLP) analysis for the *DKC1* mutation confirmed the del37L mutation in iPS lines, and karyotype analysis was normal (Fig. 1d; Supplementary Fig. 2b,c). These data show that the somatic cells from patients with a genetic impairment in telomere elongation can be reprogrammed to pluripotency.

Despite induction of endogenous *TERT* and telomerase activity (Figs. 1b,e), early passage del37L iPS cell lines displayed shorter telomeres relative to the starting fibroblast population (Fig. 1f). Addition of *TERT* to the reprogramming factors did not result in telomere elongation in del37L mutant cells (Fig. 1f), unlike in normal cells (Supplementary Fig. 3), but did increase reprogramming efficiency (Supplementary Table 1; Supplementary Text). We obtained similar results with reprogramming of an independent *DKC1* mutant line

(A386T[11]) (Fig. 1g; Supplementary Fig. 4; Supplementary Table 1). Given the telomerase dysfunction and shortened telomeres, we expected to observe limited passage of *DKC1* mutant iPS cells in culture. However, unlike the parental *DKC1* mutant fibroblasts, which senesced after 3–4 passages, we were able to continuously culture the *DKC1* mutant iPS cell lines. Compared to the early passage cells, we found by TRF analysis that telomere length in del37L iPS lines increased with continued passage (Fig. 2a). Consistent with this, despite numerous interval population doublings, late passage del37L iPS lines had telomere lengths comparable to the original fibroblast population by quantitative PCR[12] (Fig. 2b). In a blinded assessment by the complementary method of quantitative telomere fluorescence *in situ* hybridization, we confirmed that telomere length was shortened immediately after derivation but increased over time (Fig. 2c). Late passage del37L iPS cells maintained a characteristic morphology, normal karyotype, and the same clonal fingerprint as early passage cells, and reversion of the genetic mutation in *DKC1* was excluded (Supplementary Fig. 5). These data show that even in cells carrying genetic lesions that reduce telomerase function, reprogramming restores telomere elongation and self-renewal.

Previous studies have shown that reduced *TERC* levels compromise telomerase activity in *DKC1* mutant fibroblasts[11]. Ectopic expression of *TERT* alone results in telomere elongation in wild-type fibroblasts[13],[14], whereas expression of both *TERC* and *TERT* is required to restore telomere elongation in *DKC1* mutant fibroblasts[11] (Supplementary Fig. 6). We therefore investigated *TERC* levels in DC fibroblasts and iPS cells. By quantitative RT-PCR, we found that *TERC* levels in *DKC1* mutant fibroblasts were 10–15% of *TERC* levels found in wild-type fibroblasts, consistent with previous reports[10],[11] (Fig. 3a). Relative to parental fibroblasts from two patients with different *DKC1* mutations, we found *TERC* levels increased 6–8 fold in the reprogrammed derivatives, approaching levels in normal fibroblasts (Fig. 3a). In normal iPS cells, we found that *TERC* levels were approximately 3-fold higher than the fibroblasts from which they were derived (Fig. 3a). We next examined a cell line from a patient with autosomal dominant DC carrying a heterozygous 821 bp deletion in the 3' region of the *TERC* locus (DCHSF1[15],[16]). In these $TERC^{+/-}$ fibroblasts *TERC* is limiting for telomere elongation, even in the presence of exogenous *TERT*[16]. We reprogrammed the $TERC^{+/-}$ patient fibroblasts and obtained multiple independent iPS lines which all showed characteristics of pluripotency and maintained the mutant genotype (Supplementary Fig. 7). $TERC^{+/-}$ iPS cells also showed a 3-fold induction of *TERC* relative to fibroblasts (Fig. 3a), and displayed continuous self-renewal in contrast to the early senescence seen in the parental fibroblasts[16]. These data demonstrate that reprogramming of somatic cells is accompanied by upregulation of endogenous *TERC* levels, and provide a mechanism for telomere elongation and indefinite self-renewal in DC iPS cell lines (Supplementary Fig. 6).

We found that human embryonic stem (ES) cells maintain elevated *TERC* levels similar to those found in WT iPS cells (Fig. 3a), and that *TERC* levels attained in iPS cell lines derived from *DKC1* mutant, $TERC^{+/-}$ and WT cells correlated with their respective telomerase activity (Fig. 3b). Furthermore, *TERC* knockdown in DC iPS lines compromised telomere maintenance (Supplementary Fig. 8a). We found that the *TERC* locus is not amplified in DC iPS cells, and that upon differentiation of DC iPS cells, *TERC* expression reverted to the

pathologically low levels found in patient fibroblasts, and telomere length decreased (Supplementary Figs. 8b–d). Collectively, these results show that *TERC* levels are increased by reprogramming, and are a dynamically regulated and reversible property of the pluripotent state.

TERC abundance is tightly regulated by multiple transcriptional and post-transcriptional mechanisms[17,18]. To investigate transcriptional mechanisms of *TERC* upregulation, we performed chromatin immunoprecipitation (ChIP) in human iPS cells, and detected enhanced binding of Oct4 and Nanog in the *TERC* locus (Fig. 3c). These data were corroborated in murine ES cells, which likewise showed enhanced binding of Oct4 and Nanog at the *TERC* locus (Supplementary Fig. 9). However, we were unable to detect increased levels of nascent *TERC* transcription by nuclear run-off assay in iPS cells versus fibroblasts (Supplementary Fig. 10), suggesting that Oct4 and Nanog may affect transcriptional competence rather than transcriptional rate of the *TERC* locus in pluripotent cells. Additional mechanisms are required to explain the increased steady-state levels of *TERC*. To investigate post-transcriptional mechanisms of *TERC* regulation, we determined *DKC1* levels, which correlate with *TERC* levels in human cancer cells[19]. In all normal and DC iPS lines tested, we found an increase in *DKC1* transcript levels and dyskerin protein relative to the fibroblasts (Figs. 3d and e). Moreover, we found that human ES cells, like iPS cells, maintain higher levels of *DKC1* (Fig. 3d), that *DKC1* levels decreased with differentiation of iPS cells into embryoid bodies (Supplementary Fig. 11a), and that *DKC1* knockdown caused a reduction in *TERC* levels and compromised cellular viability (Supplementary Figs. 11b,c). ChIP showed binding of Oct4 and Nanog to the *DKC1* promoter in pluripotent cells (Fig. 3f), and infection of fibroblasts with retroviruses encoding the four reprogramming factors increased *DKC1* levels (Supplementary Fig. 11d). These data establish that multiple telomerase components (*TERT*, *TERC*, *DKC1*) are upregulated after reprogramming, thereby accounting for increased telomerase activity in the pluripotent state and explaining the restoration of telomere maintenance in DC iPS cells.

In an autosomal dominant DC patient carrying an 821 bp deletion in the 3' region of *TERC*, prior studies have concluded that the haploinsufficient phenotype is explained by impaired post-transcriptional accumulation of *TERC* RNA and reduced assembly of the truncated *TERC* RNA into telomerase holoenzyme[20–22] (Supplementary Fig. 12). Our ChIP data indicated Oct4 and Nanog binding in a region downstream of *TERC* that overlaps the 821 bp deletion (Fig. 3c). Moreover, we found that part of this region is predicted to have regulatory potential based on comparative genomic sequence alignment (Supplementary Fig. 13a). We hypothesized that loss of this region might compromise transcriptional activity of the deleted allele. We employed two distinct allele-specific methods to analyze the chromatin configuration in $TERC^{+/-}$ iPS cells, and in both cases found the mutant *TERC* allele to be transcriptionally inactive (Figure 4). First, allele-specific ChIP showed a striking abrogation of H3K4me3 marks and RNA polymerase II binding on the deleted allele (Fig. 4a and Supplementary Figs. 13b and 13c). Second, allele-specific DNAse I hypersensitivity analysis showed pronounced nuclease accessibility at the *TERC* promoter in normal cells (Fig. 4b) and on the normal allele in $TERC^{+/-}$ cells, but complete loss of promoter hypersensitivity on the mutant *TERC* allele (Fig. 4c and d). Collectively, these results

identify a *cis*-element in the 3' region of the *TERC* locus that appears essential for formation of a transcriptionally active chromatin structure, and suggest that mutations in this region can cause haploinsufficiency in autosomal dominant DC by diminishing *TERC* transcription (Supplementary Fig. 12).

By reprogramming somatic cells from patients with the human disease dyskeratosis congenita, we have discovered novel mechanisms of regulation of telomerase activity in the pluripotent state, thus illustrating the value of disease-specific iPS cells for basic and translational discovery. Moreover, we have shown that the RNA component of telomerase is upregulated in the pluripotent state to a degree sufficient to overcome limitations to telomere maintenance in X-linked and autosomal dominant DC. Drugs that activate the *TERC* locus may favor telomere maintenance over premature attrition in stem cell compartments where *TERT* is present but telomerase activity is limiting, such as hematopoietic stem cells[23–27], and thus might serve as therapeutic agents for bone marrow failure. Moreover, we speculate that in DC patients certain cell types such as germ cells and cancer cells, whose transcriptional programs share similarities with pluripotent cells, may also upregulate *TERC* to permit germline propagation of mutations and malignant proliferation.

Methods summary

Fibroblast lines included GM01774 (*DKC1* del37L)[11], AG04646 (*DKC1* A386T)[11], DCHSF1 ($TERC^{+/-}$ 821 bp deletion)[16] and NHSF2 (wild-type)[16]. The derivation, characterization, culture, and differentiation of iPS cells was performed as described[5]. Verification of mutations in GM01774 was as described[9]. Telomere length analysis was performed with the TeloTAGGG Telomere Length Assay kit (Roche). iPS cells were cultured feeder-free on Matrigel (Becton Dickinson) for telomerase and telomere quantitative real-time PCR (Q-PCR) assays. Telomere Q-FISH and Q-PCR were performed as described[12,28]. Telomerase activity assays were performed using the TeloTAGGG Telomerase PCR ELISA and PCR ELISA^{PLUS} kits (Roche). Detection of *TERT*, *Oct4*, *Sox2*, *Nanog*, and β *Actin* transcripts by RT-PCR was as described[5]. *TERC* and *DKC1* transcript levels were measured using Q-PCR with quantitation normalized to GAPDH. Primer sequences are provided in Methods. Chromatin immunoprecipitation was performed on BJ1, HFib2, NHSF2, and DCHSF1 iPS cells as described[29]. Antibodies and primers sequences are provided in Methods. Western blot was performed on total cellular lysates using antibodies against human dyskerin and actin (Santa Cruz). DNAse I hypersensitivity analysis was performed as described[30]. Primer sequences for probes are provided in Methods.

Methods

Cell lines and iPS derivation, characterization and culture

Fibroblast lines and iPS lines for BJ1 (ATCC); GM02416, GM04569, AG20446, GM04281, GM01390 (Coriell Cell Repository); and DH1cf subclones 16, 32, and 34 have been described[4,5,31]. GM01774 (*DKC1* del37L)[11], AG04646 (*DKC1* A386T)[11], and GM874 (ALT)[32] were also obtained from Coriell Cell Repository. DCHSF1 ($TERC^{+/-}$ 821 bp deletion) and age-matched wild-type control cells NHSF2 have been described[16].

Derivation, characterization, culture, and differentiation conditions of iPS cells have been described[31].

Retroviral and lentiviral vectors

Retroviruses encoding *TERT*, *Oct4*, *Sox2*, *Klf4*, and *c-myc* were as described[5]. The *DKC1* retroviral vector was created by cloning a full-length *DKC1* cDNA (Origene) into pMIG-W (Addgene) and retrovirus was produced as described[31]. The *TERC* lentiviral vector was created by replacing GFP pHIV7/SF-GFP[33] (a gift from Jiing-Kuan Yee) with cherry fluorescent protein and inserting a U3 promoter plus TERC from pBABE-U3-TER[11] (a gift from Kathy Collins) at an upstream site. Virus was produced by the University of Iowa Gene Vector Core.

Telomere length and telomerase assays

Using the TeloTAGGG Telomere Length Assay kit (Roche), 1–2 μg of DNA for each sample was digested and subjected to Southern analysis, and determination of mean terminal restriction fragment (TRF) length[34] was performed according to manufacturer's instructions. Briefly, autoradiographs exposed in the linear range of the hybridization signal for the lane(s) of interest were scanned with a densitometer. A volume array consisting of 30–40 quadrants was generated across the entire lane for each sample from 1–24 kb. After background subtraction, optical density (OD_i) was obtained in each of these quadrants corresponding to different DNA lengths (L_i). Mean TRF was defined as $\Sigma(OD_i)/\Sigma(OD_i/L_i)$ for each sample. To determine relative total telomeric DNA signal[34] in iPS cells versus fibroblasts, the Σ(ODi) was obtained for each lane and normalized by comparison to ethidium bromide staining of the gel or hybridization to a probe targeting a diploid somatic locus. The normalized, summated optical density value for each iPS sample was divided by that of the corresponding fibroblast line, yielding a relative signal ratio corresponding to the quantitative difference in total telomeric DNA. Telomere quantitative fluorescence *in situ* hybridization (Q-FISH) and quantitative real-time PCR (Q-PCR) were performed as described[12],[28] in a blinded fashion. For telomere Q-PCR and telomerase assays, iPS cells were cultured feeder-free on Matrigel (Becton Dickinson). Telomerase activity assays were performed using the TeloTAGGG Telomerase PCR ELISA and PCR ELISA^{PLUS} kits (Roche).

Quantitative real-time PCR (RT-PCR)

Quantitative RT-PCR was performed using SYBR green. Multiple, independent biological samples were used where available for RNA isolation using the RNeasy kit (Qiagen), and cDNA was prepared using the Superscript III First Strand Synthesis kit (Invitrogen). Detection of endogenous *TERT*, *Oct4*, *Sox2*, and β *Actin* transcripts by RT PCR was as described[5]. *TERC* and *DKC1* levels were measured using Q-PCR, with quantitation normalized to *GAPDH*, using primer pairs TRC3F/3R for *TERC* and GAPDH0.45F/0.45R for *GAPDH*, as described[35], and *DKC1*F1: (5'-ACAGGGTGAAGAGTTCTGGCACAT-3') and *DKC1*R: (5'-TGAAGGTGAGGCTTCCCAACTCAA-3') for *DKC1*.

Chromatin Immunoprecipitation (ChIP)

ChIP assay was performed on BJ1[31], HFib2[31], NHSF2 and DCHSF1 iPS cells as described[29], using anti-Oct4 (Santa Cruz; sc-8628), anti-Nanog (R&D; AF1997), anti-H3K4me3 (Abcam; ab8580), anti-RNA polymerase II (Abcam; ab817), anti-H3K27me3 (Millipore; 07–449) and anti-GFP (Santa Cruz; sc-9996). ChIP assay was performed on murine E14 ES cells using anti-Oct4 and anti-GFP antibodies above, and anti-Nanog (Cosmo Bio; REC-RCAB0002P-F).

Primer Sequences

Primers spanning the human TERC locus: Fig. 3c:

1S: (5'-CAGCACTTTGTTCTGATGAAGCCATCCC-3')

1AS: (5'-GGGTCAAGGGTATCAATGCAGAGGCTGAATAC-3')

2S: (5'-GCCTATGAATAGCACTGGGGTAGGT-3')

2AS: (5'-GCACCAAGGAGTTCAACTTGACCTCA-3')

3S: (5'-GTAGGCCTCAAACTGGTAGGATGGT-3')

3AS: (5'-CCTCCTAGCTTAGGTTGTTGATAGC-3')

4S: (5'-ACCACTCCTCCCTTACACTTTGTATGACGG-3')

4AS: (5'-GGGCTTCCTTTGTAAGGTCTGGAGTTGGTT-3')

5S: (5'-CTGGTCGAGATCTACCTTGGGAGAA-3')

5AS: (5'-AGACGTGAAGGCACCTCCAAAGTCG-3')

6S: (5'-AACCCCGGCTCACTGCCCATTCATTTT-3')

6AS: (5'-ATGCAGTTCGCTTTCCTGTTGGTGG-3')

7S: (5'-TTTCTATCCTCTGCAGACCAGACGC-3')

7AS: (5'-CGAGACAAGATTCTGCTGTAGTCAG-3')

8S: (5'-TTCCTCAGGCCTGTATCACATTTCA-3')

8AS: (5'-GGCCAAGAAACCCGATTGTCTAGAGA-3').

Fig. 4a and Supplementary Fig. 13:

DCHSF1 F: (5'-GCGAAGAGTTGGGCTCTGTCA-3')

DCHSF1 R1: (5'-CACCAACAGGAAAGCGAACTGCAT-3')

DCHSF1 R2: (5'-TCATCAGGATTCAGGCTATCACCC-3')

Primers spanning the human *DKC1* locus: Fig. 3e:

1S: (5'-TAAGAGAACTGAGAAGGCTGCG-3')

1AS: (5'-ATGGCCACTCATGATGGTTTGGGATC-3')

2S: (5'-AGCAAAGGCCTTTCAACCTCTCCGAGC-3')

2AS: (5'-TAGTTGCTTCACCTCCGGGTTTAGCTC-3')

3S: (5'-AGAGGTACTGTTTACGGAGCGTTCAGC-3')

3AS: (5'-AATGCGATTTGCTGGCTCGGCCAGTA-3')

4S: (5'-CCGAGTTGCAAGAAAGTTCTAGAGGCC-3')

4AS: (5'-GTAAGGCCAAATGTATGGGTCCCATG-3')

Primers spanning the mouse TERC locus: Supplementary Fig. S9:

1S: (5'-CCTCCCTCCACTCCCATACAGAAGG-3')

1AS: (5'-CCAAGTCTCTTTGTCCCAACTCCTC-3')

2S: (5'-CCAAATGTGACTCAGTCAATGGCACTCC-3')

2AS: (5'-GGAGGAAGTTTGGGTTGTGCTCTGTA-3')

3S: (5'-ACCACATGTGCATGTTCCTGGAGCT-3')

3AS: (5'-GCCTCTTCAGTAGCCATCATGCCTAATG-3')

4S: (5'-TATGCCACTATGTGGCTTCCACAGAAGG-3')

4AS: (5'-CCTTTCCTTCCCTCCCTTCCGGTAC-3')

5S: (5'-CATAGGGAGCTTCATCAGACTCAGTG-3')

5AS: (5'-GGCGACATTTCTCAACCAGAAGACAG-3')

6S: (5'-TCCTTGGCTTCGGTGATGTTGAGTTC-3')

6AS: (5'-CTAAGCCGGCACTCCTTACAAGGGA-3')

7S: (5'-TAAGACACCGAACACGGGGACCAGT-3')

7AS: (5'-AACGTCAGCGCAGGAGCTCCAGGTT-3')

8S: (5'-GAGAAAAACAGCGGGCGGAGAACAA-3')

8AS: (5'-ACTGGCTAGGAAGAGTGGGGAAGCG-3')

9S: (5'-CCCATCCCTTCCACACGTCAGTTCT-3')

9AS: (5'-GCAGTAGTATCTCTCGGGTTGTCCTTCA-3')

10S: (5'-GAACTTCACAATGACCATGAGCAGTCCC-3')

10AS: (5'-CCCAGAGGACATTCCTTCTAGGTTCTCTGT-3')

11S: (5'-CCAAGGCTTTGTCACTGACTGCTCA-3')

11AS: (5'-GTAGCAAGCACAGCCACCGGTGTCT-3')

12S: (5'-GTTGGTAAGATGAAGCCATCAGCCTC-3')

12AS: (5'-GGATAGTTGCCAGGCCACAGATCAAT-3')

13S: (5'-CTCTTTCTTGAATTGGACCGTGCAGG-3')

13AS: (5'-GCTTCTGGTCAGGCAGCTCATCTAAT-3')

Western analysis

Total cellular lysates were subjected to SDS-PAGE and Western transfer to PVDF membranes using standard procedures and analyzed using antibodies against human dyskerin (Santa Cruz; sc-48974) and Actin (Santa Cruz; sc-1615).

DNAse I hypersensitivity (HS) analysis

DNAse I HS analysis was performed as described[30]. Briefly, nuclei were isolated from 5×10^7 – 1×10^8 iPS cells and aliquots were subjected to treatment with various concentrations of DNAse I (Worthington), followed by lysis and phenol/chloroform extraction of DNA. Approximately 25–50 μg of DNA was digested for each lane and subjected to Southern analysis. Hybridization of PCR generated probes labelled with ^{32}P-dCTP (Ready-to-go DNA Labelling kit (-dCTP); G.E. Healthcare) was performed using Rapid-Hyb buffer (G.E. Healthcare) according to manufacturer's instructions. Primers for probes were:

Fig. 4b:

TERCNdeIF: (5'-TGTGATACAGGCCTGAGGAA-3')

TERCNdeIR: (5'-ATGCTTGCCTGGATATCTGC-3')

Fig. 4c:

TERCBsu1F: (5'-CAGGACTCGGCTCACACAT-3')

TERCBsu1R: (5'-CGATGACCATTAAAGGAACACA-3')

TERCBsu2F: (5'-GATCATCTGGGGGTAGTTGC-3')

TERCBsu2R: (5'-AAACTGAGGCTTACTGAAGCTGA-3')

TERCBsu2F/2R probe was used in Fig. 4d.

Verifications of mutations

Verification of mutations was performed by amplifying genomic DNA:

-for GM01774 (*DKC1* del37L) as described[9], using primers:

XAP101F25 (5'-ATTGCCAGAAGAAGATGTAGCC-3')

XAP101R27 (5'-TCTCTTCAGAGGATTTGAACC-3') followed by XmnI digestion; -for DCHSF1 (family DCR101)[15] as described, using primers:

HTRF2 (5'-CCTGCCGCCTTCCACCGTTCATT-3')

HTRR3 (5'-CATTACCAGCAACAGTGGACTCT-3')

-for AG04646 (*DKC1* A386T)[11] using primers:

4646F (5'-CCAGGGAGGAACCTTGTTCT-3')

4646R (5'-ACCTCCATGCTCACCTGTTC-3') followed by BstNI digestion. The primers amplify a 360 bp product flanking the mutation G1156A, resulting in loss of one of two BstNI sites.

Karyotype and DNA fingerprinting

Karyotyping and DNA fingerprinting were performed in a blinded fashion by Cell Line Genetics, Madison, WI, USA.

Clonal integration analysis by Southern blot

Oct4, *Sox2*, *Klf4*, and *c-myc*-encoding MSCV-based retroviruses, each containing an IRES-GFP cassette and a single NcoI restriction site, were used for reprogramming[31]. 10 μg of genomic DNA from iPS cells was digested with NcoI and subjected to Southern blot analysis using a GFP probe to provide a viral integration fingerprint for each clone.

TERC and *DKC1* shRNA knockdown

A duplex oligonucleotide containing an shRNA targeting the template sequence (in bold) of human *TERC*[36]:

(5'-**GTCTAACCCTAACTGAGAA**CTCGAGTTCTCAGTTAGGGTTAGACTTTTT-3') was cloned into the pLKO.1-puro vector to create pLKO-SHTR. Multiple pLKO.1-puro-based shRNA lentiviral constructs against *DKC1* were obtained from Open Biosystems, with the most effective sequence (5'-GCTCAGTGAAATGCTGTAGAA-3') targeting the 3'UTR. pLKO.1-puro-control consisted of scrambled shRNA sequences. Lentivirus containing knockdown constructs was produced by co-transfection of 293T cells with pLKO.1 constructs, psPAX2 and pMD2.G using Fugene. Supernatants were harvested, filtered, and frozen in aliquots on days 3–4 following transfection. Titres and knockdown efficiency was determined by infection of 293T cells for 8–12 hours using varying quantities

of viral supernatant and 10 μg/ml of protamine sulfate. After 24–36 hours, infected cells were selected with 2 μg/ml puromycin. RNA was harvested after 36–48 hours of selection and subjected to quantitative RT-PCR to determine knockdown efficiency of *DKC1* and *TERC*. Lentivirus constructs for knockdown of *DKC1* or *TERC* were introduced into iPS cells as follows. iPS cultures were harvested as single cells using Accutase, and 5×10^4 cells per well were plated in a 6-well plate on Matrigel (Becton Dickinson) in mTESR medium (Stem Cell Technologies) in the presence of 10 μM Y-27632 (Sigma)[37]. After 24 hours viral supernatants were added in various quantities in the presence of 10 μg/ml protamine sulfate in mTESR medium for 6 hours. After 48 hours, infected cells were selected in 0.15 μg/ml puromycin and maintained thereafter in mTESR medium with Matrigel or in conventional hES medium on DR4 puromycin-resistant feeder cells.

TERC copy number determination

TERC locus copy number in iPS relative to parental fibroblasts was determined by performing Q-PCR on genomic DNA from DCHSF1 ($TERC^{+/-}$) and del37L *DKC1* mutant fibroblasts and their iPS derivatives. Primers for the *TERC* locus were TRC3F and TRC3R[35] and for the β *Actin* locus were: ActinF: (5'- AACGGCAGAAGAGAGAACCAGTGA-3') and ActinR: (5'-TTCTACAATGAGCTGCGTGTGGCT-3'). Amplification of the *TERC* locus was normalized to that of the β *Actin* locus for each sample, and results are displayed as a ratio of normalized *TERC* signal for iPS cells relative to the parent fibroblast. Error bars denote standard error from 2 biological replicates.

Nuclear runoff transcription assay

Nuclei from 5×10^7 to 1×10^8 wild-type (NHSF2) fibroblasts or derivative iPS cells (NHSF2 iPS clone 1) were isolated and ^{32}P-labeled runoff transcripts were generated as described[38]. Labeled nascent RNA transcripts were purified using Trizol (Invitrogen) and hybridization was performed using $1–2 \times 10^6$ cpm/ml. Membranes containing hybridization targets were prepared by slot-blot of 5 μg linearized plasmid DNA targets containing full-length human *TERC* cloned into pUC19, a 439 bp fragment consisting of exon 3 of human beta-actin cloned into pUC19, or pUC19 vector alone. Hybridization was performed using Rapid-Hyb buffer (G.E. Healthcare) with pre-hybridization for 12–16 hours followed by hybridization for 48 hours.

Supplementary Material

Refer to Web version on PubMed Central for supplementary material.

Acknowledgements

This work was funded by grants from the National Institutes of Health (NIH) and the Manton Center for Orphan Disease (G.Q.D.); NIH K08HL089150, Amy Clare Potter Fellowship and Manton Center for Orphan Disease Research (S.A.); the Agency of Science, Technology and Research and the Institute of Medical Biology, Singapore (Y.H.L.); NIH R01AG0227388 (F.D.G and A.J.K.); and the James and Esther King Biomedical Research Program and MOST 973 project (2009CB941000) (D.L.K and L.L).

References

1. Kirwan M, Dokal I. Dyskeratosis congenita: a genetic disorder of many faces. Clin Genet. 2008; 73:103–12. [PubMed: 18005359]
2. Mason PJ, Wilson DB, Bessler M. Dyskeratosis congenita -- a disease of dysfunctional telomere maintenance. Curr Mol Med. 2005; 5:159–70. [PubMed: 15974869]
3. Calado RT, Young NS. Telomere maintenance and human bone marrow failure. Blood. 2008; 111:4446–55. [PubMed: 18239083]
4. Park IH, et al. Disease-specific induced pluripotent stem cells. Cell. 2008; 134:877–86. [PubMed: 18691744]
5. Park IH, et al. Reprogramming of human somatic cells to pluripotency with defined factors. Nature. 2008; 451:141–6. [PubMed: 18157115]
6. Takahashi K, et al. Induction of pluripotent stem cells from adult human fibroblasts by defined factors. Cell. 2007; 131:861–72. [PubMed: 18035408]
7. Yu J, et al. Induced pluripotent stem cell lines derived from human somatic cells. Science. 2007; 318:1917–20. [PubMed: 18029452]
8. Marion RM, et al. Telomeres acquire embryonic stem cell characteristics in induced pluripotent stem cells. Cell Stem Cell. 2009; 4:141–54. [PubMed: 19200803]
9. Heiss NS, et al. X-linked dyskeratosis congenita is caused by mutations in a highly conserved gene with putative nucleolar functions. Nat Genet. 1998; 19:32–8. [PubMed: 9590285]
10. Mitchell JR, Wood E, Collins K. A telomerase component is defective in the human disease dyskeratosis congenita. Nature. 1999; 402:551–5. [PubMed: 10591218]
11. Wong JM, Collins K. Telomerase RNA level limits telomere maintenance in X-linked dyskeratosis congenita. Genes Dev. 2006; 20:2848–58. [PubMed: 17015423]
12. Cawthon RM. Telomere measurement by quantitative PCR. Nucleic Acids Res. 2002; 30:e47. [PubMed: 12000852]
13. Bodnar AG, et al. Extension of life-span by introduction of telomerase into normal human cells. Science. 1998; 279:349–52. [PubMed: 9454332]
14. Vaziri H, Benchimol S. Reconstitution of telomerase activity in normal human cells leads to elongation of telomeres and extended replicative life span. Curr Biol. 1998; 8:279–82. [PubMed: 9501072]
15. Vulliamy T, et al. The RNA component of telomerase is mutated in autosomal dominant dyskeratosis congenita. Nature. 2001; 413:432–5. [PubMed: 11574891]
16. Westin ER, et al. Telomere restoration and extension of proliferative lifespan in dyskeratosis congenita fibroblasts. Aging Cell. 2007; 6:383–94. [PubMed: 17381549]
17. Cairney CJ, Keith WN. Telomerase redefined: integrated regulation of hTR and hTERT for telomere maintenance and telomerase activity. Biochimie. 2008; 90:13–23. [PubMed: 17854971]
18. Yi X, Tesmer VM, Savre-Train I, Shay JW, Wright WE. Both transcriptional and posttranscriptional mechanisms regulate human telomerase template RNA levels. Mol Cell Biol. 1999; 19:3989–97. [PubMed: 10330139]
19. Montanaro L, et al. Dyskerin expression influences the level of ribosomal RNA pseudo-uridylation and telomerase RNA component in human breast cancer. J Pathol. 2006; 210:10–8. [PubMed: 16841302]
20. Fu D, Collins K. Distinct biogenesis pathways for human telomerase RNA and H/ACA small nucleolar RNAs. Mol Cell. 2003; 11:1361–72. [PubMed: 12769858]
21. Marrone A, Stevens D, Vulliamy T, Dokal I, Mason PJ. Heterozygous telomerase RNA mutations found in dyskeratosis congenita and aplastic anemia reduce telomerase activity via haploinsufficiency. Blood. 2004; 104:3936–42. [PubMed: 15319288]
22. Trahan C, Dragon F. Dyskeratosis congenita mutations in the H/ACA domain of human telomerase RNA affect its assembly into a pre-RNP. RNA. 2009; 15:235–43. [PubMed: 19095616]
23. Broccoli D, Young JW, de Lange T. Telomerase activity in normal and malignant hematopoietic cells. Proc Natl Acad Sci U S A. 1995; 92:9082–6. [PubMed: 7568077]

24. Chiu CP, et al. Differential expression of telomerase activity in hematopoietic progenitors from adult human bone marrow. Stem Cells. 1996; 14:239–48. [PubMed: 8991544]
25. Hiyama K, et al. Activation of telomerase in human lymphocytes and hematopoietic progenitor cells. J Immunol. 1995; 155:3711–5. [PubMed: 7561072]
26. Allsopp RC, Morin GB, DePinho R, Harley CB, Weissman IL. Telomerase is required to slow telomere shortening and extend replicative lifespan of HSCs during serial transplantation. Blood. 2003; 102:517–20. [PubMed: 12663456]
27. Kirwan M, et al. Exogenous TERC alone can enhance proliferative potential, telomerase activity and telomere length in lymphocytes from dyskeratosis congenita patients. Br J Haematol. 2008
28. Liu L, et al. Telomere lengthening early in development. Nat Cell Biol. 2007; 9:1436–41. [PubMed: 17982445]
29. Loh YH, et al. The Oct4 and Nanog transcription network regulates pluripotency in mouse embryonic stem cells. Nat Genet. 2006; 38:431–40. [PubMed: 16518401]
30. Agarwal S, Rao A. Modulation of chromatin structure regulates cytokine gene expression during T cell differentiation. Immunity. 1998; 9:765–75. [PubMed: 9881967]
31. Park IH, Lerou PH, Zhao R, Huo H, Daley GQ. Generation of human-induced pluripotent stem cells. Nat Protoc. 2008; 3:1180–6. [PubMed: 18600223]
32. Bryan TM, Englezou A, Gupta J, Bacchetti S, Reddel RR. Telomere elongation in immortal human cells without detectable telomerase activity. EMBO J. 1995; 14:4240–8. [PubMed: 7556065]
33. Yam PY, et al. Design of HIV vectors for efficient gene delivery into human hematopoietic cells. Mol Ther. 2002; 5:479–84. [PubMed: 11945076]
34. Harley CB, Futcher AB, Greider CW. Telomeres shorten during ageing of human fibroblasts. Nature. 1990; 345:458–60. [PubMed: 2342578]
35. Atkinson SP, Hoare SF, Glasspool RM, Keith WN. Lack of telomerase gene expression in alternative lengthening of telomere cells is associated with chromatin remodeling of the hTR and hTERT gene promoters. Cancer Res. 2005; 65:7585–90. [PubMed: 16140922]
36. Li S, et al. Rapid inhibition of cancer cell growth induced by lentiviral delivery and expression of mutant-template telomerase RNA and anti-telomerase short-interfering RNA. Cancer Res. 2004; 64:4833–40. [PubMed: 15256453]
37. Watanabe K, et al. A ROCK inhibitor permits survival of dissociated human embryonic stem cells. Nat Biotechnol. 2007; 25:681–6. [PubMed: 17529971]
38. Greenberg ME, Bender TP. Identification of newly transcribed RNA. Curr Protoc Mol Biol. 2007; Chapter 4(Unit 4):10. [PubMed: 18265405]

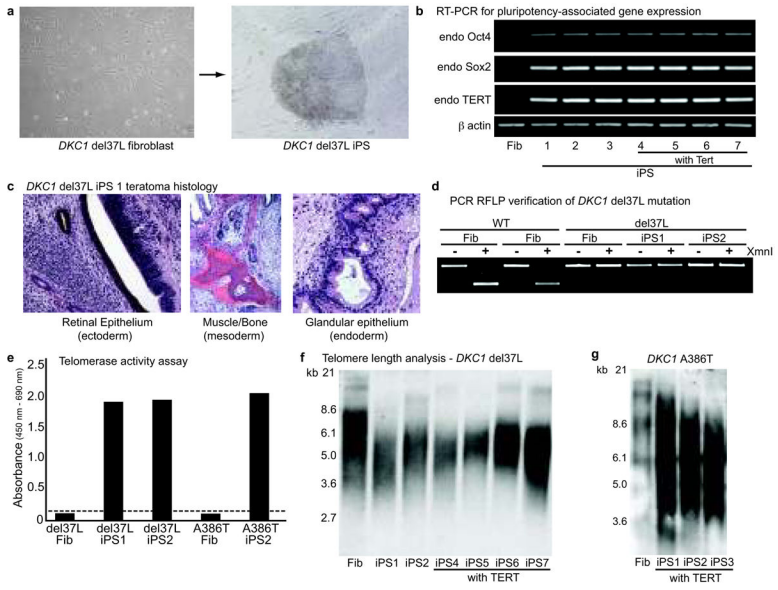

Figure 1. Derivation and characterization of *DKC1* mutant iPS cells

a, *DKC1* del37L fibroblasts and iPS colony. **b,** RT-PCR for endogenous ("endo") *Oct4*, *Sox2*, *TERT*, and *Actin* transcripts in del37L fibroblasts (Fib) and iPS cells derived with and without exogenous Tert. **c,** Histology of del37L iPS1 teratomas. **d,** PCR RFLP verification of del37L mutation in iPS clones. **e,** Telomerase activity assay in *DKC1* mutant iPS lines (dash = background). **f,** Telomere Southern blot in *DKC1* del37L fibroblasts and early passage iPS clones. **g,** Telomere Southern blot in *DKC1* A386T fibroblasts and early passage iPS clones.

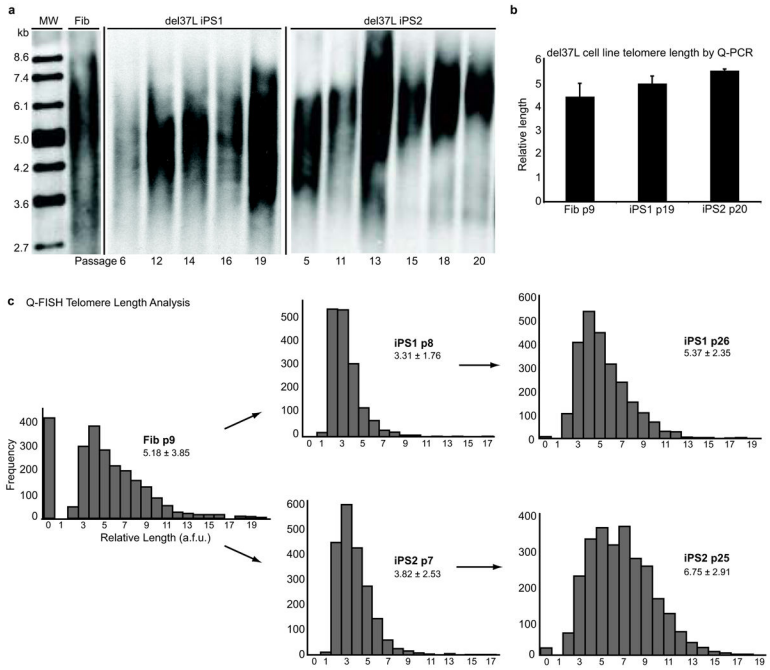

Figure 2. Telomere elongation in *DKC1* mutant iPS cells

a, Telomere Southern blot of del37L fibroblasts (Fib) and iPS clones 1 and 2 as a function of passage. **b,** Quantitative real-time PCR (Q-PCR) analysis of telomere length in del37L fibroblasts and iPS clones at indicated passages (p). Error bars represent s.e.m. **c,** Quantitative fluorescence *in situ* hybridization (Q-FISH) for telomere length in del37L cells. a.f.u. = arbitrary fluorescence units. Inset: mean relative length values shown +/− s.d.

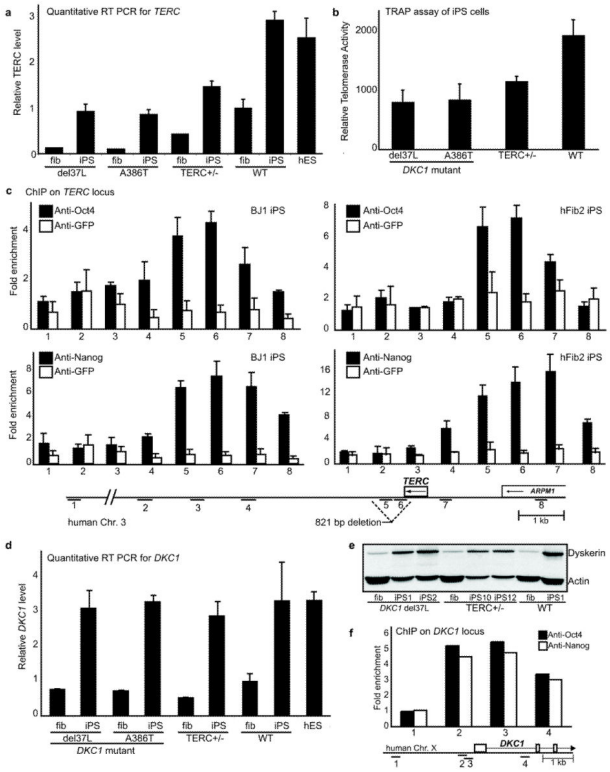

Figure 3. Upregulation of *TERC* and *DKC1* in iPS cells

a, Q-PCR measurement of *TERC* transcripts in *DKC1* mutant, *TERC*$^{+/-}$, and wild-type (WT) fibroblasts (fib) and iPS cells, and human ES (hES) cells, normalized to *GAPDH* and relative to WT fibroblasts. **b,** Quantitative TRAP assay in iPS cells. **c,** ChIP of the human *TERC* locus in WT iPS cells. 821 bp deletion in *TERC*$^{+/-}$ cells is indicated. **d,** Q-PCR measurement of *DKC1* transcripts (as in **a**). **e,** Western blot of dyskerin and actin in WT and DC fibroblasts and iPS clones. **f,** ChIP of the *DKC1* locus (see map) in WT iPS cells. All error bars represent s.e.m.

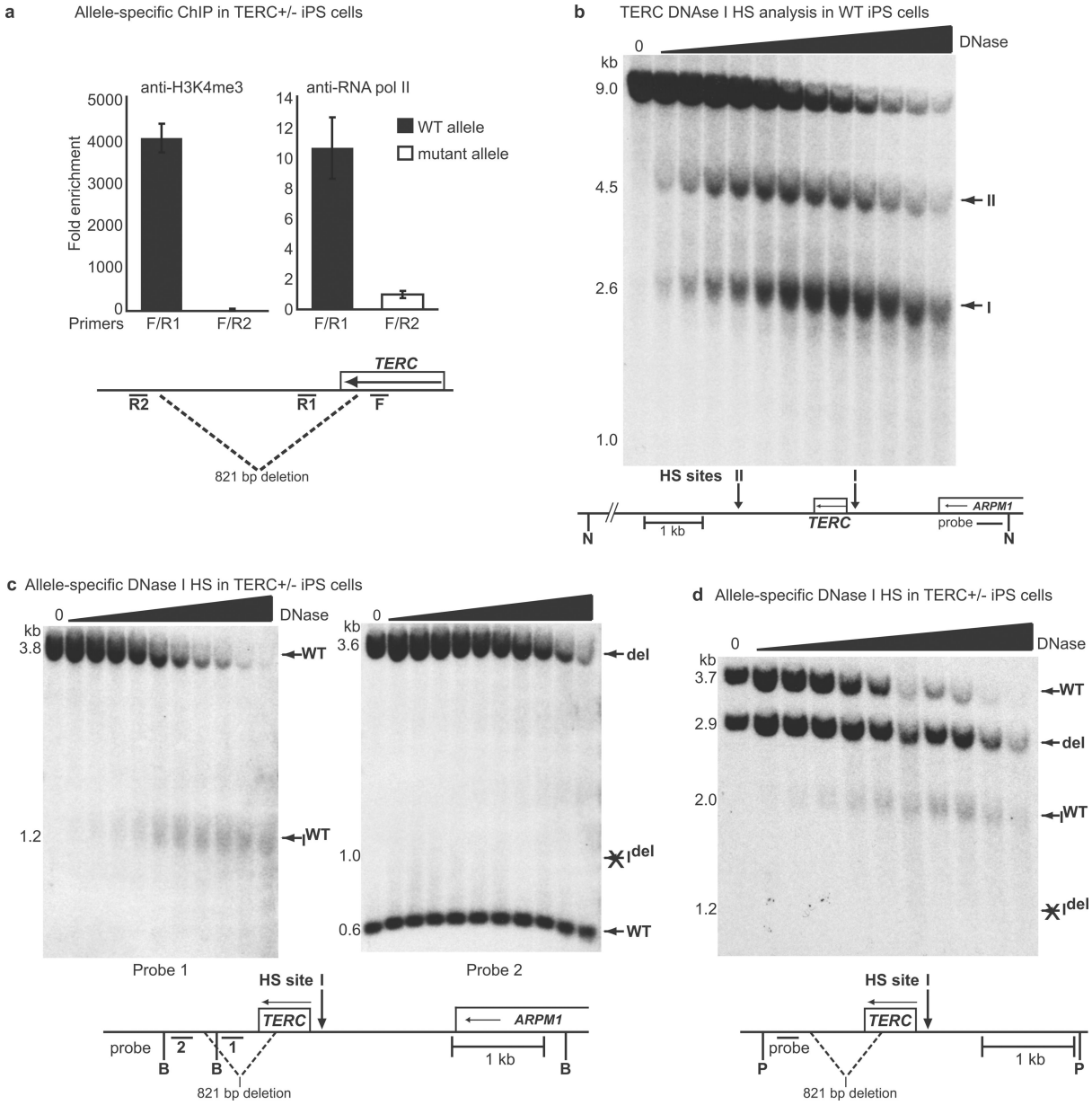

Figure 4. Transcriptional silencing is associated with a 3' deletion in the TERC locus

a, ChIP using *TERC*$^{+/-}$ iPS cells with allele-specific primers (F / R1 for WT; F / R2 for mutant). Error bars represent s.e.m. **b,** DNAse I hypersensitivity (HS) analysis probing a *TERC* locus NdeI (N) fragment in WT iPS cells, showing two discrete HS sites. **c,** Allele-specific DNAse I HS analysis probing *TERC* locus Bsu36I (B) fragments in *TERC*$^{+/-}$ iPS cells (probe 1 assesses WT parent allele and HS site I (I^{WT}); probe 2 assesses both parent alleles (WT and del) but HS I only on the deleted allele (I^{del})). **d**, As in **c**, with PflMI (P) digestion and indicated probe for simultaneous assessment of both WT and deleted parent alleles and HS sites.